Physical Biology

PAPER

Epidemic spreading in an expanded parameter space: the supercritical scaling laws and subcritical metastable phases

Gaetano Campi[1,2,*], Antonio Valletta[3], Andrea Perali[2,4], Augusto Marcelli[2,5] and Antonio Bianconi[1,2,6]

[1] Institute of Crystallography, CNR, via Salaria Km 29. 300, Monterotondo Stazione, Roma I-00015, Italy
[2] Rome International Centre Materials Science Superstripes RICMASS via dei Sabelli 119A, 00185 Rome, Italy
[3] Institute for Microelectronics and Microsystems, IMM, Consiglio Nazionale delle Ricerche CNR Via del Fosso del Cavaliere 100, 00133 Roma, Italy
[4] School of Pharmacy, Physics Unit, University of Camerino, 62032 Camerino (MC), Italy
[5] INFN—Laboratori Nazionali di Frascati, 00044 Frascati (RM), Italy
[6] National Research Nuclear University MEPhI (Moscow Engineering Physics Institute), 115409 Moscow, Russia
[*] Author to whom any correspondence should be addressed.

E-mail: gaetano.campi@ic.cnr.it, antonio.bianconi@ricmass.eu, antonio.valletta@artov.imm.cnr.it, andrea.perali@unicam.it and augusto.marcelli@lnf.infn.it

RECEIVED
10 January 2021

REVISED
22 April 2021

ACCEPTED FOR PUBLICATION
26 May 2021

PUBLISHED
21 June 2021

Keywords: coronavirus epidemics with containment measures (CEwCM), physical laws of epidemics evolution, power law relation between doubling-time and reproductive number

Abstract

While the mathematical laws of uncontrolled epidemic spreading are well known, the statistical physics of coronavirus epidemics with containment measures is currently lacking. The modelling of available data of the first wave of the Covid-19 pandemic in 2020 over 230 days, in different countries representative of different containment policies is relevant to quantify the efficiency of these policies to face the containment of any successive wave. At this aim we have built a 3D phase diagram tracking the simultaneous evolution and the interplay of the doubling time, T_d, and the reproductive number, R_t measured using the methodological definition used by the Robert Koch Institute. In this expanded parameter space three different main phases, *supercritical*, *critical* and *subcritical* are identified. Moreover, we have found that in the *supercritical* regime with $R_t > 1$ the doubling time is smaller than 40 days. In this phase we have established the power law relation between T_d and $(R_t - 1)^{-\nu}$ with the exponent ν depending on the definition of reproductive number. In the *subcritical* regime where $R_t < 1$ and $T_d > 100$ days, we have identified arrested metastable phases where T_d is nearly constant.

1. Introduction

While the mean-field theory of intrinsic dynamics of uncontrolled epidemics is well known [1, 2], nowadays the scientific discussion is focusing on the dynamics of *epidemics with containment measures* [2–5], addressing the role of extrinsic effects due to the spatio-temporal evolution of contact networks [6–9]. In this work we verify proposed mathematical laws driving coronavirus 2020 epidemics with containment measures (called here CEwCM). Different epidemiology protocols such as *lockdown, case finding, mobile tracing* (LFT) [10–16] and *lockdown stop and go* (LSG) [17–19] has been applied by different countries.

While many works [20–30] have analyzed short-time intervals of the CEwCM, here we analyse the full-time window of the first Covid-19 wave in: (i) South Korea, which applied the LFT policy compared with (ii) Italy and (iii) United States of America which applied the LSG policy with strict and loose rules, respectively. We have verified the physical laws of the time evolution of the CEwCM [24–30] using a new 3D expanded parameter space $T_d(t, R_t)$: where T_d and R_t are the time-dependent doubling and reproductive number.

In CEwCM time evolution three main regimes are clearly identified: *supercritical, critical* and *subcritical.* The regimes *supercritical*, with $R_t > 1$ and *subcritical* with $R_t < 1$ are defined in epidemic spreading theories in references [4, 5]. In a previous work [10] we have considered the critical regime occurring when $1 < R_t < 1.1$. Correspondingly, it was found that the time dependent T_d values are $T_d < 40$ days in the

supercritical phase, $T_d > 100$ in the *subcritical* phase and $[40 < T_d < 100]$ in the *critical* phase.

We have verified here that in the first wave the supercritical phase is characterized by the $T_d = C_K(R_t - 1)^{-\nu}$ power law function of the variable doubling time T_d versus the reproductive number R_t. The key point of this work is the use of the log–log plots of T_d versus $(R_t - 1)$ to understand the time evolution of coronavirus in different countries adopting different containment policies. Finally, we provide a quantitative comparison of the Covid-19 first and second wave evolution in Italy compared with South Korea and USA.

2. Methods

The data for each country have been taken from the recognized public data base *OurWorldInData* [31]. We have extracted, first, the time-dependent doubling time T_d from the curve of total infected cases, $Z(t)$, and, second, the time-dependent reproductive number R_t from the curve of active infected cases, $X(t)$, using the methodological definition provided by the Robert Koch Institute [31]. Thus, the strategy in our methodological approach has been the extraction of two time dependent parameters (1) the doubling time, T_d, and (2) the reproduction number, R_t, from two independent datasets: T_d has been extracted from the total cases while R_t has been obtained from the active cases.

2.1. The basic doubling time T_{d0} and basic reproductive number R_0

Figure 1(a) shows a pictorial view of the viral epidemic spreading starting with the uncontrolled epidemic in the early days of the outbreak with a *basic reproductive number* $R_0 = 2$ and the basic doubling time $T_{d0} = 2$ days (which separates successive nth generations with 2^n infected persons). In the early days the cumulative curve of the total number of cases $Z(t)$ increases exponentially with a characteristic rate α

$$Z(t) = Z(0)\, e^{\alpha t} = Z(0)\, 2^{\frac{t}{T_{d0}}} \tag{1}$$

therefore, the *basic doubling time*

$$T_{d0} = \frac{\log(2)}{\alpha} \tag{2}$$

has been quickly extracted by several groups showing that it is in the range $2 < T_{d0} < 2.8$ days with $2 < R_0 < 3$, as reported in several works. [19]

2.2. Time evolution law of the time-dependent doubling time T_d and reproduction number R_t in the 3D phase diagram $T_d(t, R_t)$

As the epidemic goes forward, the total number of cases $Z(t)$ will include both the active cases and the removed (recovered) individuals. The time evolution of the epidemics modified by extrinsic effects of the containment measures is tracked by the time-dependent doubling time, T_d. The time-dependent T_d of coronavirus 2020 epidemics is obtained by fitting the cumulative curve $Z(t)$ over a five days period centered at $t \pm \Delta t$ with $\Delta t = 2$ days. T_d has been evaluated by taking the time derivative of the cumulative curve $Z(t)$ over five days of the logarithm of the cumulative infection curve $\frac{d}{dt}\log(Z(t)) = \alpha(t) = \frac{\log(2)}{T_d(t)}$ that leads to

$$T_d(t) = \frac{\log(2)}{\frac{d}{dt}\log(Z(t))}. \tag{3}$$

The time-dependent variable reproductive number R_t can be measured by different methods [2–7, 32–34]. In this work we have used the model independent procedure proposed by the Robert Koch Institute [33], where R_t is the ratio of the actually infected individuals $X(t)$ at time t divided by the actually infected individuals at the time $(t - \Delta t)$:

$$\boldsymbol{R_t(t)} = \frac{\boldsymbol{X(t)}}{\boldsymbol{X(t - \Delta t)}}. \tag{4}$$

The relationship between the time-dependent doubling time T_d and the reproductive number R_t as defined by the Robert Koch Institute [33] can be derived by considering that

$$Z(t + \Delta t) = 2^{\frac{\Delta t}{T_d}} Z(t) = \exp\left(\log(2)\frac{\Delta t}{T_d}\right) Z(t) \cong \left(1 + \log(2)\frac{\Delta t}{T_d}\right) Z(t) \tag{5}$$

,where the equality holds true if $\Delta t < T_d$.

Hence, we find that

$$R_t(t) - 1 = \log(2)\frac{\Delta t}{T_d(t)} \tag{6}$$

and

$$T_d(t) = C_K(R_t(t) - 1)^{-1} \tag{7}$$

with $C_K = \Delta t \log(2)$.

3. Results and discussion

3.1. The three-dimensional parameter space $T_d(t, R_t)$

Figure 1(b) shows the expanded three-dimensional parameter space $T_d(t', R_t)$ proposed in this work. The joint plot of T_d, and R_t calculated as a function of time provides an exhaustive description of the epidemic spreading during the time interval $t' = t - t_0 = 230$ days, where t_0 is the day onset of the first wave of Covid-19 outbreak in the three studied countries. The gray slab indicates the critical regime where $40 < T_d < 100$ days and $R_{t*} \sim 1$. Around the time t^* the curve of the active infected cases $X(t)$ of the Covid-19 epidemic wave reaches the maximum of

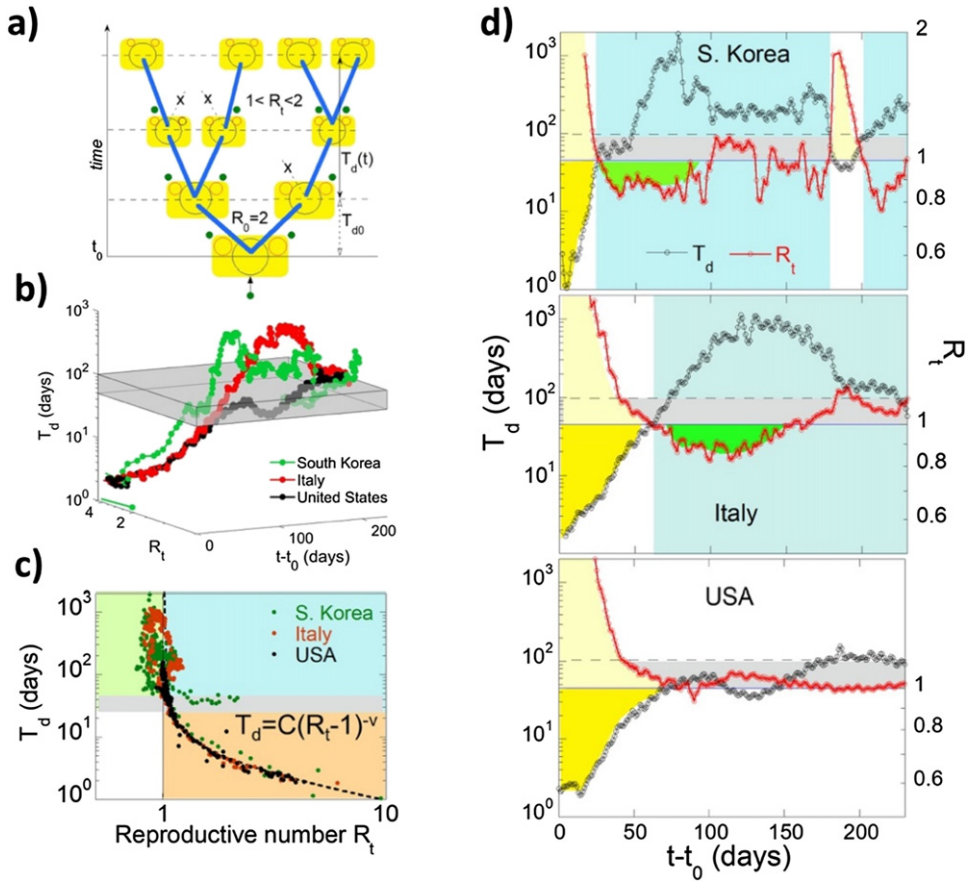

Figure 1. (a) Pictorial view of the epidemic growth starting with basic reproductive number, R_0, and basic doubling time, T_{d0}. Containment measures in the supercritical phase of epidemic spreading reduce the reproductive number R_t and lengthen the doubling time T_d. (b) The 3D phase diagram where the doubling time $T_d(t', R_t)$ is plotted as a function of $t' = t - t_0$ and the effective reproductive number R_t for South Korea (green) Italy (red) and USA (black). The gray space indicates the critical crossover where $40 < T_d < 100$ days separates the supercritical phase ($T_d < 40$ days; $R_t > 1$) from the subcritical phase ($T_d > 100$ days; $R_t < 1$). (c) Log–log plot of doubling time T_d vs R_t in the three countries. In the orange supercritical regime all curves of the three countries are fitted by the function $T_d = C(R_t - 1)^{-\nu}$, with exponent $\upsilon = 0.7$. The data in the subcritical regime, green area, where $T_d > 100$ days and $R_t < 1$, show the incoherent disordered behaviour. The critical phase is confined within the horizontal gray dashed strip where $40 < T_d < 100$ days. (d) T_d and R_t as a function of $t' = t - t_0$ in the three selected countries. In the supercritical regime in the yellow areas the doubling time (gray curve) increases in the range $2 < T_d < 40$ days and the reproductive number R_t decreases down to 1. In the subcritical phases, indicated by the light blue areas, T_d increases to a maximum and R_t decreases up to a minimum and it extends up to the point where they cross again in the critical regime. The green area identifies the subcritical regime for $R_t < 1$ and $T_d > 100$ days where the epidemic spreading is arrested. Finally, the gray area identifies the critical regime where $1 < R_t < 1.1$ and $40 < T_d < 100$ days.

a dome. The critical zone separates the *supercritical* regime from the *subcritical* regime.

The *supercritical* regimes occurs in the lower part of figure 1(b) characterized by a shorter doubling time $T_d < T_d(t^*) = 40$ days, for $t' < t^*$ and a larger reproductive number $R_t > 1$ which occurs where the curve of the active infected cases $X(t)$ is growing. The *subcritical* regime occurs in the upper part of figure 1(b) where $T_d > 100$ days and $R_t < 1$, i.e. where the curve $X(t)$ is decreasing. Figure 1(c) shows the projection of the 3D plot in the T_d–R_t plane for the three considered countries. This figure allows us to verify that in the supercritical regime (orange area) $T_d(R_t)$ follows the universal power law of equation (8) characterized by the divergence of $T_d(R_t)$ while approaching $R_t = 1$ (thick dotted line).

Figure 1(c) shows that in the orange supercritical regime all curves of the three countries are fitted by the function $T_d(t) = C(R_t(t) - 1)^{-\nu}$ with $\nu = 0.7$.

In the subcritical phase we see a random distribution of the data pairs (T_d, R_t) in the green area. The critical phase is indicated by the full gray slab as in the 3D plot of figure 1(b), which corresponds to the range [40–100] days of the doubling time T_d and the reproductive number in the range $1 < R_t < 1.1$. The *supercritical* regime is indicated by the yellow areas, ranging from the outbreak threshold time t_0 and the day t^*, where $T_d(t^*)$ reaches the value of 40 days. The straight line T_d in the semi-logarithm scale in the yellow region shows that in the *supercritical* regime, the doubling time T_d follows the universal exponential law [10, 27]

$$T_d(t) = A\, e^{(t-t_0)/s} \tag{8}$$

where t_0 is the time of the onset of the outbreak and s (called the s-factor) is the characteristic time of the applied containment policy [10, 27]. In some countries, particularly those where the mitigation measures were not strict, we do not observe an initial exponential growth [35, 36]. This is not the case of Covid-19 pandemic in the considered countries where data analysis show a clear exponential behavior described by equation (8).

Figure 1(d) shows both T_d and R_t vs the time $t' = t - t_0$ for each country. The upper panel shows that the time lapse interval of the supercritical phase $t^* - t_0 = 24$ days for the yellow region of South Korea is related with the small s-factor (6–7 days) which are both a factor 2.5 shorter than the s-factor of Italy and USA where $60 < (t^* - t_0) < 70$ days, which imply a time duration of the first wave lockdown a factor 2–3 longer.

The subcritical phase occurs when T_d becomes larger than 100 (light blue areas) and R_t drops below 1 (green areas). In this phase the data (green area in Figure 1c) show the incoherent disordered behavior. The critical phase is confined within the horizontal gray dashed strip where $40 < T_d < 100$ days.

Italy reached a well-defined subcritical phase extending in the green area due to the enforced strict rules of the imposed lockdown. On the contrary, the plot shows that in USA, where loose rules for the lockdown have been applied, the transition to the subcritical regime has been stopped, and the country remained for a very long time in the critical phase. This approach shows that the subcritical phase in South Korea remained close to the critical phase and faced a second Covid-19 very short wave indicated by the yellow area. We underline that the second wave in South Korea lasted only 20 days with a doubling time longer than 40 days. The shape of the second wave in South Korea clearly shows the efficiency of the applied contact tracing to keep the spreading under control, to reduce the lockdown to a minimum time and to reduce the number of fatalities.

3.2. The relation between the reproductive number R_t and T_d in our work and in alternative approaches

The attempts to fit the pandemic data available for the different countries by using the SIR model with estimations for τ_i and τ_r values that are inferred from clinical studies have failed to reproduce the experimental trends. The reason is that the SIR model is too simplistic, using a time independent τ_i and τ_r to reproduce quantitatively the trend of the different pandemic curves in the presence of different containment policies. There are several factors that determine a deviation of the trend predicted by the SIR model from the experimental one. As an example: the presence of asymptomatic individuals (not reported in experimental data) that are capable of spreading the infections could be accounted in a susceptible–infected–removed (SIR) model by 'overestimating' the infective capability of the symptomatic individuals. Moreover the SIR model fails to give account of the experimental data because of the negligible variation of the susceptible population during the first wave in the three countries investigated in this work. The varation of the susceptible population $S(t)$ at the end of the first wave normalized to the maximum value $S(0)$ at the threshold of epidemic breakout are given by

$1 - S(t)/S(0) = 1 - (60\,360\,000 - 317\,000)/60360\,000 = 0.0053$ in Italy;

$1 - S(t)/S(0) = 1 - (330\,775\,889 - 7589\,957)/330\,775\,889 = 0.0229$ in USA

$1 - S(t)/S(0) = 1 - (50\,599\,528 - 92\,817)/50\,599\,528 = 0.0018$ in South Korea.

Therefore, the maximum variation of the susceptible population reported by the data bases are 0.53%, 2.3% and 0.18% for Italy, USA and South Korea, respectively.

In this scenario several authors have discusses the Covid-19 epidemics with containment measures using the susceptible–infected model [4].

Barabasi in his book [7] has considered the Susceptible–Infected–Susceptible model where the number of infected cases in the endemic state is $I(\infty) = 1 - \mu/\beta(k)$, and he found the relation between the characteristic time of a pathogen $\tau = 1/\mu(R_0 - 1)$ and $(R_0 - 1)$ where $R_0 = \beta(k)/\mu$ is the basic reproductive number which is similar to our equation (7).

Some authors have proposed an unconventional inverted SIR model [25, 26] where the susceptible population (S) is assumed to be constant. In this non conventional epidemological model the values of the extracted infection τ_i and recovery time τ_r do not agree with clinical data, but have to be considered only as the extracted effective values of τ_i and τ_r by solving ('inverting') the SIR model. Therefore the effective R_e number extracted by the ratio between τ_i and τ_r parameters, given by the inverted SIR model, deviates from the standard epidemiological definitions.

The values of τ_i and τ_r extracted using the inverted SIR model show a very large variation with time which quantify the effect of the containment measures that have been adopted and are different from the 'clinical' τ_i and τ_r. [37]

The $T_d(t, R_e)$ phase diagram, where the effective reproduction time, namely R_e, is extracted by the inverted SIR theory [25, 26] is shown in figure 2. The panel (a) in figure 2 shows that the transition from the supercritical to the subcritical regime is driven by the joint increase of τ_i and decrease of τ_r. The opposite occurs when the subcritical to the supercritical transition happens in metastable phases at end of the first wave and the threshold of the second wave. In figures 2(b) and (c) a similar analysis is performed on the epidemic data of Italy and USA respectively. The comparison among countries shown in figures 2(a)

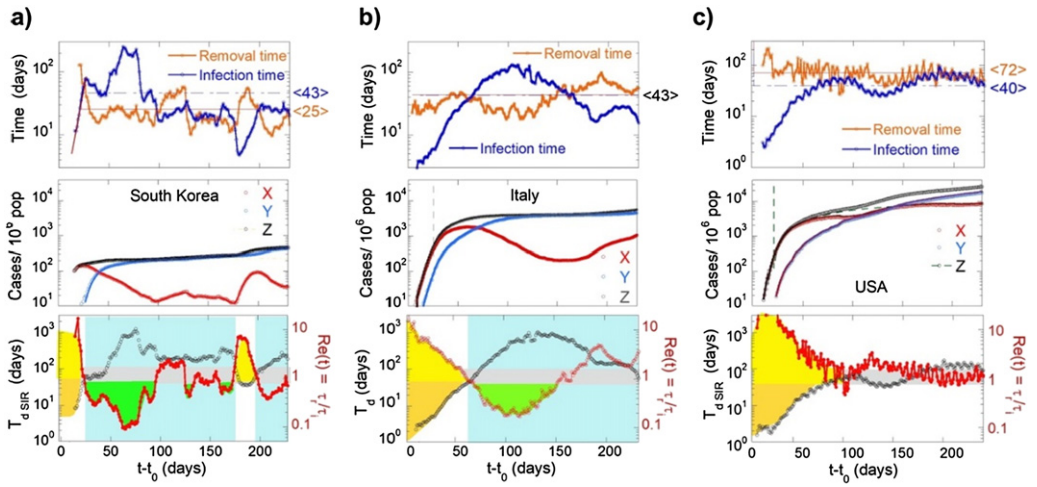

Figure 2. The unconventional R_e and T_d extracted by the inverted SIR model in the limit of a nearly constant susceptible population during the first wave applied to (a) South Korea, (b) Italy and (c) USA. The upper panels show the extracted (red) effective removal time τ_r and (blue) infection time τ_i as a function of $t - t_0$. In the middle panels, we report the curves of cases per million population, of infected (X) (red), removed Y (blue) and total cases ($Z = X + Y$) (black) as a function of time. The $Z(t)$ curve follows the Ostwald law [10, 27] (dashed line) characteristic of ordering growth in heterogeneous systems [35–37]. In the lower panels we show T_d and unconventional effective R_e as extracted by the inverted SIR model to be compared with figure 2(c) showing the T_d and R_t extracted in this work. The shaded light blue area indicates the subcritical phase separating the first and the second Covid-19 wave. In Italy this subcritical phase occurs for $60 < t' < 230$ days. In USA there is no evidence for the presence of a subcritical regime, the yellow supercritical phase is followed by the critical phase in the gray strip extending over a large time interval.

and (b), 1(c) indicates different efforts in testing and tracing. The cumulative curve $Z(t)$ of the total number of cases of the epidemics in the supercritical phase, slows down approaching the critical regime, where it has been fitted by the complex Ostwald growth law [10, 17, 38–40]

$$Z(t - t_0) = C\left\{1 - e^{-(t-t_0)/\tau}\right\} \cdot (t - t_0)^{\gamma} \qquad (9)$$

which is a mixed exponential and power-law behavior determined by nucleation of different phases and ordering phenomena in complex multiphase systems out of equilibrium [38–40]. The onset of this behavior, obtained by best curve fitting, is reported by the dashed lines in the central panels of figure 2.

The time-dependent doubling time given by

$$T_d(t) = \frac{\log(2)}{\frac{d}{dt}\log(Z(t))} = \frac{\log(2)}{\frac{\frac{d}{dt}Z(t)}{Z(t)}} \qquad (10)$$

can be obtained from the equation for $\tau_i(t)$. I In the framework of the SIR model, we obtain the following expression for T_d

$$T_d(t) = \log(2)\,\tau_i(t)\,\frac{Z(t)}{X(t)} \qquad (11)$$

$$T_d(t) = \log(2)\,\tau_r(t)\,\frac{Z(t)}{X(t)}\frac{1}{R_e(t)}. \qquad (12)$$

The doubling time T_d calculated using equation (12), has been plotted in figure 2 with the effective reproduction number R_e, computed within the inverted SIR model. The $T_d(t)$ curve estimated with the inverted SIR model agrees with the T_d curve estimated from the epidemic data (shown in the lower panels of figure 2).

At variance the effective R_e curves exhibit differences from the reproductive number R_t obtained in this work using the Robert Koch Institute method shown in figure 1. Nevertheless, the time where the critical regime occurs, i.e. when both R_t and R_e are equal is the same in the predictions by the inverted SIR approach.

The large value of $\tau_r \approx 100$ days during the early days or during the whole period have to be interpreted as the lack of testing and tracing cases, not certainly as the presence of individuals that are capable to transfer the infections for a such long time.

3.3. The universal power law relation between time-dependent doubling time, T_d, and reproduction number, R_t, in the supercritical phase

Log–log plot of the doubling time T_d as a function of $R_t - 1$ and $R_e - 1$ in the three countries are compared in the upper and lower panels of figure 3. The R_t values are higher than R_e calculated with inverted SIR method. Although the difference, the T_d vs $R_t - 1$ behavior in the two approach appears qualitatively similar. We get the critical exponent $\nu = 1$, using $R_e - 1$ extracted by the mean-field inverted SIR model.

We have used R_t as defined by the Robert Koch Institute method with $\Delta t = 5$ days which gives a values of R_t in qualitative agreement with other methods. [34] Fitting the data we have found

$$T_d(t) = C_K(R_t(t) - 1)^{-\nu} \qquad (13)$$

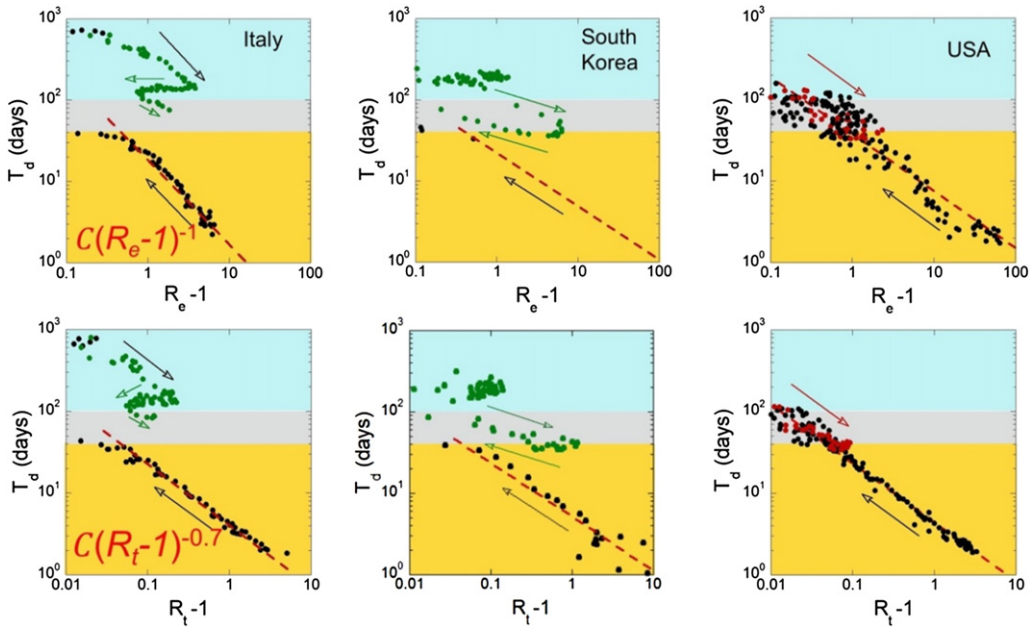

Figure 3. Log–log plot of doubling time T_d in three countries as a function of $R_t - 1$ extracted by the inverted SIR model (upper panels) and by the Robert Koch Institute empirical method (lower panels). Black dots in the yellow region indicate T_d in the supercritical regime which follows the universal analytical power law function $[T_d = C(R_t - 1)^{-\nu}]$ of a divergent T_d approaching $R_t = 1$ fitted by the red dashed lines. The critical exponent ν is 1 in the inverted SIR model (upper panels) and 0.7 using Robert Koch prescriptions with 5 days interval (lower panels). The critical phase is described by the horizontal gray strip where $40 < T_d < 100$ days. The green dots in the blue light area indicate the metastable states in the subcritical regime where the epidemic spreading growth is arrested $T_d > 40$ days also if $R_t > 1$. While the metastable state in Italy in the subcritical (green dots) with $T_d =$ constant indicates a precursor of the second wave regime in South Korea the loop of the curve (green dots) in the critical regime (gray strip) is determined by the second wave shown in the lower panel of figure 2(a). In USA the epidemic spreading never entered in the subcritical phase and reversible oscillations (R_t decreasing is inducted by red dots) and are observed in the critical regime.

with the exponent $\nu \approx 0.7 \pm 0.05$ in the three studied countries. We have estimated R_t with the Robert Koch Institute method [33] using different time intervals $\Delta t = 3$, 5, 7, 9, 11, and 21 days. Afterwards we have fitted the data $T_d(R_t)$ using equation (13) in the three selected countries using R_t measured with the different time intervals Δt. We have found that the exponent ν decreases by increasing the time interval Δt following the stretched exponential function $\nu = e^{-(\Delta t/\tau)^{\beta}}$ with $\tau = 24.5$ days and $\beta = 0.8$ shown in figure 4. Therefore, $\nu \to 1$ for $\Delta t \to 0$ as predicted by equation (7) in agreement with the mathematical limit for the exponent extracted by the Robert Koch Institute method for the time interval $\Delta t \to 0$.

This result is particularly relevant to predict the onset of new epidemic waves. The onset of the supercritical phase of successive wave will be easily detected in the $[T_d, R_t - 1]$ or $[T_d, R_e - 1]$ diagram when dots move towards the yellow area, where the supercritical regime will be following the universal power law of equation (7). Figure 3 shows that in USA the epidemics never entered in the subcritical phase and the it has been fluctuating in the critical phase with an increasing (black dots) and decreasing (red dots) doubling time along with the predictions of the power law. The rapidly aborted second wave in South Korea is well depicted by the green dots forming the loop in figure 3, where the containment policy succeeded to push up the doubling-time avoiding its following down toward the universal power law growth rate of the first Covid-19 wave.

3.4. Metastable phases and the second wave in Italy

In figure 3 the phase diagram of epidemic spreading in Italy during the first wave shows the gray strip corresponding to the *critical* regime above the *supercritical* orange area, and below the *subcritical* regime. As previousely mentioned, in this *subcritical* phase the T_d vs R_t values show a non-analytical disordered distribution (see also figure 1(c)), while in the supercritical regime it is described by the analytical universal power law of equation (7). The green dots in the T_d vs R_t plots in figure 3 show that the subcritical phase occurs also for cases where $T_d > 100$ although $R_t > 1$. When put on a lattice, the SIR model depends on the geometry of contacts, and is in the same universality class as ordinary percolation. R_t is essentially the percolation threshold for the SIR mean-field model, in fact infection can grow without bound where R_t is greater than 1 on a Erdős–Rényi network or a Bethe lattice [41], while there is no percolation for R_t less than 1. However, making the network composed of closed loops which attenuate the probability of an epidemic, different complex geometries [42], and in presence of long range interactions the percolating epidemic

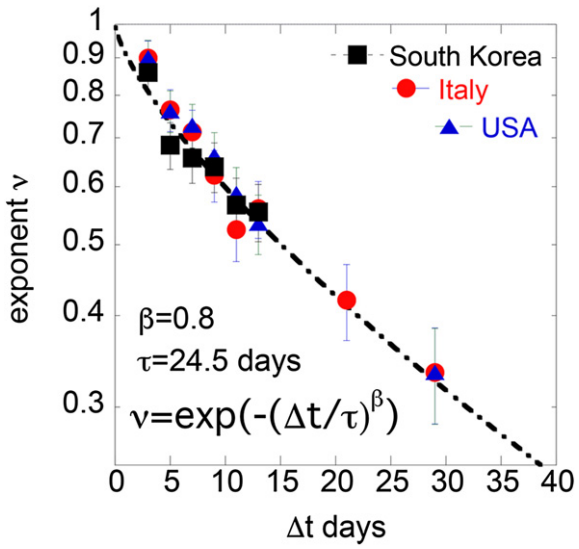

Figure 4. The figure shows the exponent ν in the curve $T_{\rm d}\,(t) = C_K(R_t\,(t) - 1)^{-\nu}$ of the doubling time $T_{\rm d}$ versus R_t in the supercritical regime, as a function of the time lapse interval Δt, used to extract R_t using the Koch Institut phenomenological method. Different time lapse intervals Δt in the range $3 < \Delta t < 30$ days have been used from the epidemiological data for South Korea USA, and Italy to calculate R_t. The exponent ν as a function of the time lapse interval Δt (used to calculate R_t) follows a stretched exponential law $\nu = {\rm e}^{-(\Delta t/\tau)^{\beta}}$ with $\tau = 24.8$ days and $\beta = 0.8$ showing that $\nu = -1$ in the limit $\Delta t \to 0$ days.

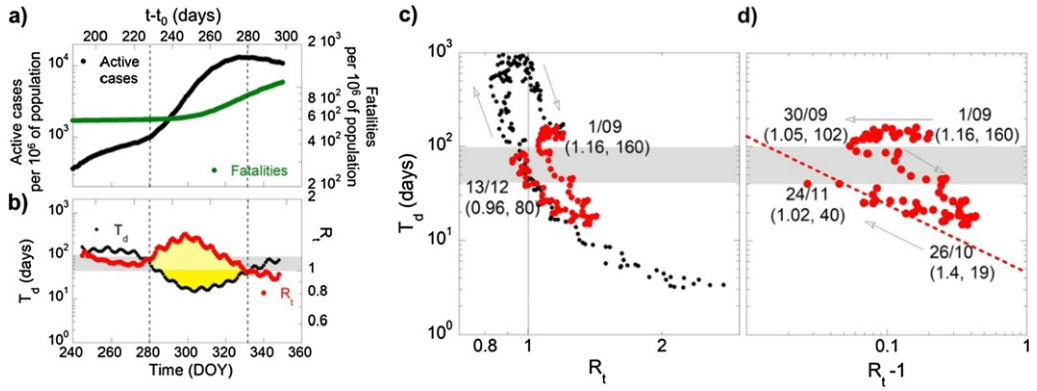

Figure 5. Panel (a) the curve of the active infected cases and fatalities per million populations as a function of time during the second wave in Italy. The time is measured by the day of the year 2020 in the lower scale, and the time $t' = t - t_0$ from the onset of outbreak in Italy in the upper x scale. Panel (b) shows $T_{\rm d}$ and R_t for the second wave in Italy with the same scale as in figure 1 for the first wave in Italy. The yellow area indicates the explosive percolating epidemic regime of the second wave in Italy. Panel (c) shows the $T_{\rm d}$ versus R_t plot of the second wave (red dots) compared with the first wave (black dots) panel (d) shows the log–log plot of $T_{\rm d}$ versus $(R_t - 1)$. The red dots in the second wave shows the first uncontrolled increase of R_t and decrease of $T_{\rm d}$ up to its peak in the time lapse interval $274 < {\rm DOY} < 300$ which is followed by the coronavirus epidemics controlled by containment measures in the time range $300 < {\rm DOY} < 330$ which follows the power law given by equation $T_{\rm d}\,(t) = C_K(R_t\,(t) - 1)^{-\nu}$ with $\nu = 0.7$.

threshold $R_t{}^*$ could be as large as about 1.5. [43, 44] The plot of the Italian case unveils the unexpected arrested metastable phases for $1.06 < R_t < R_t{}^* = 1.2$ with a decreasing reproduction number at constant doubling-time (R_t decreases while $T_{\rm d}$ remains constant) as indicated by horizontal arrows in the curve (green dots) of the ($T_{\rm d}$ vs R_t) plot.

After the flat metastable state in the subcritical phase at the end of the first wave on October 7, 2020 the doubling time decreased toward the supercritical regime at the end of the zig-zag behavior where the arrows indicate the time direction. In figure 3 the data of South Korea at the end of the flat regime show that the efficient mobile contact tracing elevated the doubling time. On the contrary in Italy the poor contact tracing method here enforced caused the decreasing of the doubling time with the onset of supercritical regime of the second Covid-19 epidemic wave.

The evolution of the second epidemic wave in Italy between September 1 and December 13, is plotted in figure 5. The data in panel (b) of figure 3 and the data in figure 5 overlap in the time measured in days of year (DOY) for the period September 1 (245 DOY)

and October 7 (281 DOY) where we have observed the metastable arrested phase discussed above which can be considered either as the end of the first wave as well as the onset of the second wave. Panel (a) of figure 5 shows the time lapse interval where the curve of active cases has shown its maximum increasing rate due to the second wave in Italy. In the three panels it is possible to see that from DOY 275 (October 1) to DOY = 300 (October 26) the reproductive number increased from 1.05 to 1.4 while the doubling-time decreased from $T_{\rm d} = 102$ days in the sub-critical regime to $T_{\rm d} = 19$ days in the supercritical regime. The rate of the growth rate of active cases started to decrease only after DOY = 300 (October 26). It is remarkable that in the time period 300 < DOY < 330 days, when some strict containment rules have been enforced, the CEwCM developed again as in the same regime of the first wave following both equation (7) $T_{\rm d}(t) = C_K(R_t(t) - 1)^{-\nu}$ and equation (8) $T_{\rm d}(t) = A\,{\rm e}^{(t-t_0)/s}$ where the s factor is about two times larger than in the South Korea second wave shown in figure 3.

4. Conclusions

The results of this work provide an original quantitative approach for understanding the time evolution of the Covid-19 pandemic. We show that it is necessary to expand the parameter space, monitoring the evolution of the pair of relevant variables ($T_{\rm d}$, R_t). By expanding the parameter space it became possible to analyze in a more precise and complete manner the data of the epidemics, probing and tuning at the same time containment measures. This work sheds light and provides new quantitative experimental tools for the quantitative statistical physics of this Covid-19 pandemic, but certainly also to face future epidemic events thanks to its predicting power.

The results of our work can be summarized as follows: the joint analysis of the *doubling time* $T_{\rm d}$, i.e. the time it takes for the number of infected individuals to double in value extracted from the cumulative curves of total (infected plus removed) cases, combined with the reproductive number R_t, i.e. the average number of infected persons by a single positive case, extracted from the cumulative curves of the number of active infected cases, provide complementary information on the efficiency of the applied containment policies. Therefore, the proposed approach could be used to dynamically control and to improve the effects of mitigation policies.

Author contributions

The authors equally contributed to this work.

Competing interest statement

Authors declare that they have no competing interests.

Acknowledgments

We acknowledge financial support of Superstripes onlus non-profit association for scientific culture

Data availability statement

The data that support the findings of this study are available upon reasonable request from the authors.

ORCID iDs

Gaetano Campi https://orcid.org/0000-0001-9845-9394
Antonio Valletta https://orcid.org/0000-0002-3901-9230
Andrea Perali https://orcid.org/0000-0002-4914-4975
Augusto Marcelli https://orcid.org/0000-0002-8138-7547
Antonio Bianconi https://orcid.org/0000-0001-9795-3913

References

[1] Kermack W O, McKendrick A G and Walker G T 1927 A contribution to the mathematical theory of epidemics *Proc. R. Soc.* A **115** 700–21
[2] Anderson R M and May R M 1991 *Infectious Diseases of Humans: Dynamics and Control* (Oxford: Oxford University Press)
[3] Peak C M, Childs L M, Grad Y H and Buckee C O 2017 Comparing nonpharmaceutical interventions for containing emerging epidemics *Proc. Natl Acad. Sci. USA* **114** 4023–8
[4] Bianconi G and Krapivsky P L 2020 Epidemics with containment measures *Phys. Rev.* E **102** 032305
[5] Radicchi F and Bianconi G 2020 Epidemic plateau in critical susceptible-infected-removed dynamics with nontrivial initial conditions *Phys. Rev.* E **102** 052309
[6] Pastor-Satorras R, Castellano C, Van Mieghem P and Vespignani A 2015 Epidemic processes in complex networks *Rev. Mod. Phys.* **87** 925
[7] Barabási A L 2016 *Network Science* (Cambridge: Cambridge University Press)
[8] Bianconi G 2018 *Multilayer Networks: Structure and Function* (Oxford: Oxford University Press)
[9] Bell J *et al* 2020 Beyond covid-19: network science and sustainable exit strategies *J. Phys. Complex.* **2** 021001
[10] Bianconi A, Marcelli A, Campi G and Perali A 2020 Efficiency of covid-19 mobile contact tracing containment by measuring time-dependent doubling time *Phys. Biol.* **17** 065006
[11] Park Y J *et al* 2020 Contact tracing during coronavirus disease outbreak, South Korea, 2020 *Emerg. Infect. Dis.* **26** 2465–8
[12] Sun K and Viboud C 2020 Impact of contact tracing on SARS-CoV-2 transmission *Lancet Infect. Dis.* **20** 876–7
[13] Lai S *et al* 2020 Effect of non-pharmaceutical interventions to contain covid-19 in China *Nature* **585** 410–3

[14] Ferretti L, Wymant C, Kendall M, Zhao L, Nurtay A, Abeler-Dörner L, Parker M, Bonsall D and Fraser C 2020 Quantifying SARS-CoV-2 transmission suggests epidemic control with digital contact tracing *Science* **368** eabb6936
[15] Bianconi G, Sun H, Rapisardi G and Arenas A 2020 A message-passing approach to epidemic tracing and mitigation with apps (arXiv:2007.05277)
[16] Kim H and Paul A 2020 Contact tracing: a game of big numbers in the time of COVID-19 (arXiv:2004.10762)
[17] Anderson R M, Heesterbeek H, Klinkenberg D and Hollingsworth T D 2020 How will country-based mitigation measures influence the course of the covid-19 epidemic? *Lancet* **395** 931–4
[18] Verity R *et al* 2020 Estimates of the severity of coronavirus disease 2019: a model-based analysis *Lancet Infect. Dis.* **20** 669–77
[19] Biggerstaff M *et al* 2020 Early insights from statistical and mathematical modeling of key epidemiologic parameters of covid-19 *Emerg. Infect. Dis.* **26** e201074
[20] Matrajt L and Leung T 2020 Evaluating the effectiveness of social distancing interventions to delay or flatten the epidemic curve of coronavirus disease *Emerg. Infect. Dis.* **26** 1740
[21] Gatto M, Bertuzzo E, Mari L, Miccoli S, Carraro L, Casagrandi R and Rinaldo A 2020 Spread and dynamics of the covid-19 epidemic in Italy: effects of emergency containment measures *Proc. Natl Acad. Sci. USA* **117** 10484–91
[22] Fanelli D and Piazza F 2020 Analysis and forecast of covid-19 spreading in China, Italy and France *Chaos Solitons Fractals* **134** 109761
[23] Sebastiani G, Massa M and Riboli E 2020 Covid-19 epidemic in Italy: evolution, projections and impact of government measures *Eur. J. Epidemiol.* **35** 341
[24] Cadoni M 2020 How to reduce epidemic peaks keeping under control the time-span of the epidemic *Chaos Solitons Fractals* **138** 109940
[25] Sun H, Qiu Y, Yan H, Huang Y, Zhu Y, Gu J and Chen S X 2020 Tracking reproductivity of covid-19 epidemic in China with varying coefficient SIR model *J. Data Sci.* **18** 455–72
[26] Chen Y C, Lu P E, Chang C S and Liu T H 2020 A time-dependent SIR model for covid-19 with undetectable infected persons *IEEE Transactions on Network Science and Engineering* **7** 3279–94
[27] Bianconi A, Marcelli A, Campi G and Perali A 2020 Ostwald growth rate in controlled covid-19 epidemic spreading as in arrested growth in quantum complex matter *Condens. Matter* **5** 23
[28] Knafo W 2020 Covid-19: monitoring the propagation of the first waves of the pandemic *4open* **3** 5
[29] Ziff R M and Ziff A L 2020 Fractal kinetics of covid-19 pandemic *International Journal* **6** 43–69
[30] Blasius B 2020 Power-law distribution in the number of confirmed covid-19 cases *Chaos* **30** 093123
[31] Max R, Hannah R, Esteban O-O and Joe H 2020 Coronavirus pandemic (COVID-19) Published online at OurWorldInData.org. Retrieved from: 'https://ourworldindata.org/coronavirus' [Online Resource]
[32] Wallinga J and Lipsitch M 2006 How generation intervals shape the relationship between growth rates and reproductive numbers *Proc. R. Soc. B.* **274** 599–604
[33] Robert Koch Institute 2020 *Epidemiologisches Bulletin 17* (Accessed 23 April 2020) https://rki.de/DE/Content/Infekt/EpidBull/Archiv/2020/Ausgaben/17_20.pdf?__blob=publicationFile
[34] Annunziatio A and Asikainen T 2020 *Effective Reproduction Number Estimation from Data Series, EUR 30300 EN* (Luxembourg: Publications Office of the European Union)
[35] Tsallis C and Tirnakli U 2020 Predicting COVID-19 peaks around the world *Front. Phys.* **8** 217
[36] Thurner S, Klimek P and Hanel R 2020 A network-based explanation of why most COVID-19 infection curves are linear *Proc. Natl Acad. Sci. USA* **117** 22684–9
[37] Hu Z *et al* 2020 Clinical characteristics of 24 asymptomatic infections with COVID-19 screened among close contacts in Nanjing, China *Sci. China Life Sci.* **63** 706–11
[38] Poccia N *et al* 2012 Optimum inhomogeneity of local lattice distortions in La_2CuO_{4+y} *Proc. Natl Acad. Sci.* **109** 15685–90
[39] Campi G, Mari A, Amenitsch H, Pifferi A, Cannas C and Suber L 2010 Monitoring early stages of silver particle formation in a polymer solution by *in situ* and time resolved small angle x-ray scattering *Nanoscale* **2** 2447–55
[40] Poccia N, Fratini M, Ricci A, Campi G, Barba L, Vittorini-Orgeas A, Bianconi G, Aeppli G and Bianconi A 2011 Evolution and control of oxygen order in a cuprate superconductor *Nat. Mater.* **10** 733–6
[41] Grassberger P 1983 On the critical behavior of the general epidemic process and dynamical percolation *Math. Biosci.* **63** 157–72
[42] Tome T and Ziff R M 2010 Critical behavior of the susceptible-infected-recovered model on a square lattice *Phys. Rev.* E **82** 051921
[43] Schlosser F, Maier B F, Jack O, Hinrichs D, Zachariae A and Brockmann D 2020 COVID-19 lockdown induces disease-mitigating structural changes in mobility networks *Proc. Natl Acad. Sci. USA* **117** 32883–90
[44] Ziff R M 2021 Percolation and the pandemic *Phys.* A **568** 125723